Thermal Diffusivity Measurement of High-Conductive Materials by means of Dynamic Grating Radiometry[1]

Y. Taguchi[2] and Y. Nagasaka[2, 3]

[1] Paper presented at the Fourteenth Symposium on Thermophysical Properties, June 25-30, 2000, Boulder, Colorado, U.S.A.

[2] Department of Mechanical Engineering, Keio University, 3-14-1, Hiyoshi, Yokohama, 223-8522, Japan.

[3] To whom correspondence should be addressed.

ABSTRACT

A new apparatus based on a dynamic grating radiometry (DGR) to measure thermal diffusivity of high-conductive materials such as graphite and diamond has been developed. In DGR method, a sample surface is heated by interference of two pulsed laser beams, and the decay of temperature at a spot on the thermal grating is monitored by an infrared detector. In the ideal case where the grating period is much smaller than the light absorption length, the thermal diffusivity parallel to the surface can be determined from the decay constant and the grating period. This paper describes a procedure to extract the thermal diffusivity parallel to the plane with eliminating the effect of anisotropy and the preliminary measurement using Zr foil. A quadratic dependence of time constant on fringe space has been observed in the fringe space change. Data are also presented for a 0.1 mm thick graphite-sheet. The results indicate the capability of DGR to measure the anisotropic high-conductive materials.

KEY WORDS: anisotropic graphite-sheet; high-conductive materials; dynamic grating radiometry; thermal diffusivity.

1. INTRODUCTION

Recently, electronic packaging of high power devices or very densely packed integrated circuits such as ULSI have brought about some serious thermal problems. As one of the ways to solve the problems, high-conductive materials like a CVD diamond (thermal diffusivity is about 1000 $mm^2 \cdot s^{-1}$) has lately attracted considerable attentions and will promise to solve the problems for heat sink. In the production process of high-conductive thin materials, the film will have an anisotropy between parallel and perpendicular to the plane. However, the study of contact-free thermal diffusivity measurements, which is for anisotropic high-conductive materials *in situ* condition, is not enough under existing circumstances. Therefore, simultaneous measurement technique of thermal diffusivity parallel and perpendicular to the plane *in situ* condition is required for the thermal design in local region.

Graebner [1] developed the transient thermal grating method (TTG), which is the measurement technique for the thermal diffusivity parallel to the plane. In TTG, the thermal diffusivity is detected by the pulsed-laser excitation and thermal radiation detection of a thermal grating on a sample surface. Graebner measured the horizontal thermal properties of CVD diamond films by means of TTG. However, the thermal diffusivity perpendicular to the plane is not considered in TTG so that it is difficult to detect the anisotropy of the sample. We have adopted the idea of TTG and extended the theory of two-dimensional heat conduction and developed a procedure to analyze the thermal diffusivity parallel to the plane which avoid the influence of anisotropy problem. In the present paper, we discuss the validity of dynamic grating radiometry (DGR) [2, 3] to measure anisotropic thermal diffusivity through the preliminary measurement for Zr foil. According to the results of experimental measurements for graphite-sheets, we verify the capability of DGR to measure high-conductive orthotropic materials.

2. PRINCIPLE OF MEASUREMENT

2.1 Two-Dimensional Heat Conduction Model

The principle of DGR follows that the transient temperature of the thermal grating is expressed by the heat conduction both parallel and perpendicular to the plane as shown in Fig. 1. If the light absorption length is much larger than the grating period (volume heating), the assumption of one-dimensional heat conduction parallel to the plane (x-direction) is satisfied (Fig. 1 (a)). On the other hand, if the light absorption length is much smaller than the grating period (surface heating), one-dimensional heat conduction perpendicular to the plane (z-direction) is permissible in a small area (Fig. 1 (b)). In reality, we need to know the two-dimensional heat conduction process to measure the thermal diffusivity from infrared signal of transient temperature decay.

To solve the heat conduction equation, the Green's function [4] as the temperature at (x, y, z) at the point (x', y', z') at the time τ is adopted. The Green's function is most conveniently defined for the closed surface as the potential which vanishes over the surface. For any of the boundary conditions, the solution for the two-dimensional region can be expressed as the product of the corresponding one-variable simpler solutions. In this case, the exact shape of temperature distribution in the x-axis and z-axis is described by

$$T_{xz}(x, z, t) = \int G_x \cdot \Psi(x')\, dx' \cdot \int G_z \cdot \Psi(z')\, dz' \,, \tag{1}$$

where G is the Green's function for each direction, Ψ the initial temperature distribution which is excited by heating laser beams. The each term of Eq. (1) means

$$T_x(x, t) = \int G_x \cdot \Psi(x')\, dx' \,, \tag{2}$$

$$T_z(z, t) = \int G_z \cdot \Psi(z')\, dz' \,. \tag{3}$$

Eq. (2) is the temperature distribution parallel to the plane, and Eq. (3) is the temperature distribution perpendicular to the plane, respectively. Hence, the two-dimensional heat conduction problem is dealt with individual axis.

The assumptions of one-dimensional heat conduction parallel to the plane are as follows. (1) The sample thickness is semi-infinite value. ($-\infty < x < \infty$, $0 < z$) (2) There is no inner heat source in the sample. (3) The grating period Λ is much smaller than the laser beam diameter. The initial temperature distribution which is produced by the interference of two laser beams can be written

$$T(x, 0) = T_0 + T_1 \cos(kx)\,, \tag{4}$$

where T_0 is the mean initial temperature rise, T_1 the spatially periodic temperature distribution and $k = 2\pi / \Lambda$ the wave number of the fringe. The solution of the appropriate heat conduction equation is described as follows.

$$T_x(x, t) = T_0 + T_1 \exp\left(-\frac{t}{\tau_x}\right) \cos\left(\frac{2\pi}{\Lambda}x\right), \tag{5}$$

where

$$\tau_x = \frac{1}{a_x}\left(\frac{\Lambda}{2\pi}\right)^2. \tag{6}$$

τ_x is the relaxation time of heat conduction, which implies that the spatially temperature distribution decays exponentially. The time decay of the signal is related inversely proportional to the thermal diffusivity a_x and directly to the square of the fringe space Λ^2.

In the case of heat conduction for the z-direction, assumptions of initial states are as follows. (1) The sample is semi-infinite value. ($-\infty < x < \infty$, $0 < z < \infty$) (2) The surface is heated uniformly. (3) The sample surface boundaries are adiabatic. By using the initial temperature Ψ, the temperature at z at the time t can be written as Eq. (3). In this case of vertical heat conduction, the Green's function G_z in a sample is given by

$$G_z = \frac{1}{2\sqrt{\pi\, a_z\, t}}\left[\exp\left\{\frac{-(z-z')}{4\, a_z\, t}\right\} + \exp\left\{\frac{-(z+z')}{4\, a_z\, t}\right\}\right]. \tag{7}$$

The initial temperature distribution in the z-direction $\Psi(z)$ is given by the following equation.

$$\Psi(z) = \exp(-\alpha z), \tag{8}$$

where α is absorption coefficient. The temperature distribution at z at the time t is given by Eqs. (3), (7), and (8). Then,

$$T_z(0, t) = \exp\left(\frac{t}{\tau_z}\right) \operatorname{erfc}\left(\sqrt{\frac{t}{\tau_z}}\right), \tag{9}$$

where $\tau_z = 1 / (a_z \cdot \alpha^2)$ is time constant to z-direction and a_z the thermal diffusivity perpendicular to the plane and erfc (x) the complementary error function.

Then, substituting Eqs. (5) and (9) for Eq. (1), the solution of two-dimensional heat conduction applicable to DGR is expressed as follows.

$$T_{xz}(0, 0, t) = \left\{T_0 + T_1 \exp\left(-\frac{t}{\tau_x}\right)\right\}\left\{\exp\left(\frac{t}{\tau_z}\right) \operatorname{erfc}\left(\sqrt{\frac{t}{\tau_z}}\right)\right\}. \tag{10}$$

As mentioned above, the relative temperature rise which is obtained as Eq. (10) includes the information of two-dimensional heat conduction.

2.2 A Procedure to Extract a_x from Two-Dimensional Condition

In real DGR measurement, it is difficult to perform experiment under the condition with negligible heat flow in z-direction. Therefore, in the present study, to analyze the signal which includes information of two-dimensional heat conduction, thermal diffusivity parallel and perpendicular to the plane are determined separately.

To separate the thermal diffusivity parallel and perpendicular to the plane, the pattern of thermal sinusoidal distribution, which is obtained by scanning the interference pattern on the sample surface, is utilized. Fig. 2 shows the temperature distribution on a sample surface heated by an interference pattern. Defined point A as a peak and point B as a valley of a thermal grating, the temperature distribution of the infrared detector outputs when the off-axis paraboloidal reflectors spot is located on the both extremes are described as

$$T_P(0,\,0,\,t) = \left\{T_0 + T_1 \exp\left(-\frac{t}{\tau_x}\right)\right\}\left\{\exp\left(\frac{t}{\tau_z}\right) \operatorname{erfc}\left(\sqrt{\frac{t}{\tau_z}}\right)\right\}, \tag{11}$$

$$T_V\left(\frac{\Lambda}{2},\,0,\,t\right) = \left\{T_0 - T_1 \exp\left(-\frac{t}{\tau_x}\right)\right\}\left\{\exp\left(\frac{t}{\tau_z}\right) \operatorname{erfc}\left(\sqrt{\frac{t}{\tau_z}}\right)\right\}, \tag{12}$$

where T_P and T_V are temperature decay of the peak and the valley, respectively. Then, the heat conduction in z-direction is separated by using the peak (Eq. (11)) and valley (Eq. (12)) of thermal grating as follows.

$$T_z = \frac{1}{2}\left\{T_P(0,\,0,\,t) + T_V\left(\frac{\Lambda}{2},\,0,\,t\right)\right\} = T_0 \exp\left(\frac{t}{\tau_z}\right) \operatorname{erfc}\left(\sqrt{\frac{t}{\tau_z}}\right). \tag{13}$$

Hence, the horizontal temperature distribution T_x can be expected such as

$$T_z = \frac{T_P}{(T_P + T_V)\,/\,2} = 1 + \frac{T_1}{T_0} \exp\left(-\frac{t}{\tau_x}\right). \tag{14}$$

Fig. 3, which is a typical data detected by the infrared detector, explains the temperature distribution of point A and B. Using the temperature distribution of peak and valley, the non-dimensional temperature change which includes information of horizontal thermal diffusivity is calculated by Eq. (14). Thus, in DGR, we can obtain the thermal diffusivity parallel to the plane which eliminates the influence of vertical heat conduction problem.

By using the simplex-method [5], the experimental data can be fitted to Eq. (14) to calculate a_x.

3. EXPERIMENTAL APPARATUS

Fig. 4 schematically exhibits the present experimental apparatus. The transient thermal gradient is created by a Nd:YAG laser (wave length 532 nm) whose power is 50 mJ / 5 ns with repetition rate of 10 Hz Q-switch. Pulsed high-power laser beam is divided by a beam splitter into two beams of equal intensity. Two beams are intersected on the sample surface by mirrors under an angle θ (θ is determined as an interval of M3 and M5) and generate an optical interference fringe pattern whose intensity distribution is spatially sinusoidal. In order to monitor the decay of temperature distribution which is caused by the heat conduction process, we employ infrared thermometry by measuring the thermal radiation emitted from a spot on the surface. To scan the sample surface, the nano-order moving system which shifts the position of heated area on the sample is adopted. The off-axis paraboloidal mirrors (the spatial resolving diameter δ is estimated 100 ~ 250 μm) condense the emission from a sample to LN-cooled HgCdTe infrared detector (Kolmar Tech., Inc. : KV104-0.05-A-3-SMA) and the weak signal is amplified by a preamplifier (band width of 16 MHz). The detected signal is averaged for a hundred of laser pulses to significantly improve the S/N ratio.

Considered as one optical measurement for the anisotropic thermal diffusivity, the characteristics of DGR are summarized as follows. (1) To consider two-dimensional heat conduction, thermal diffusivity parallel and perpendicular to the plane are calculated. (2) Quick detection system in DGR can measure the fast decay of surface temperature in high-conductive material. (3) The signal is detected by infrared so that DGR can be applied to the sample having not so smooth surface like a graphite-sheet (surface roughness is about 2 μm).

4. RESULTS AND DISCUSSIONS

4.1 Preliminary Measurement Using Zr Foil

In order to check the validity of the present apparatus and the data analysis procedure, we have measured the thermal diffusivity of isotropic Zr foil of 50 μm thickness. A quadratic dependence of time constant on fringe space is observed from 0.261 mm to 0.464 mm change in fringe space. Fig. 3 exhibits a typical data detected by the infrared detector and Fig. 5 shows the corresponding derived non-dimensional temperature change T_x from the measurement. As can be seen from Fig. 5, S/N ratio is inferior due to the nature of the present calculation procedure. This may be improved by re-designing of amplifier or averaging the signal at the digital oscilloscope. Because of spatial resolving power arising from off-set paraboloidal reflectors and instability of YAG pulsed beam, V_{det} (visibility detected by infrared detector) is quite frequently smaller than V_{CCD} (visibility detected by CCD camera). Hence, improvement of the S/N ratio requires the increasing of the visibility. The quadratic dependence of decay time and fringe space is shown in Fig. 6. The time constant, which is calculated by the analysis of two-dimensional heat conduction model, is proportional to square of the fringe space. Consequently, the applicability of the principle and the present instrumentation of DGR are confirmed.

4.2 Experiment Using Graphite-Sheet

To confirm the capability of the present DGR apparatus for high-conductive material, the graphite-sheet is employed. The graphite-sheet has high conductivity and anisotropy between parallel and perpendicular to the plane (Table I) [6]. For measuring the thermal diffusivity of graphite-sheet, the fringe space is widened to obtain longer decay time constant. Considered about time dependence on fringe space, Fig. 7 shows the time constant on each gratings (Λ = 545.6 mm and 430.3 mm). The decay time is fitted to quadratic dependence on fringe space. The thermal diffusivity of graphite-sheet is calculated as 602 $mm^2 \cdot s^{-1}$ by analyzing the slope of Fig. 7. Besides, we considered the verification analysis of anisotropy (section 2.3). In the experiment of Zr foil, the vertical thermal diffusivity to the plane is impossible to calculate because the heat flow perpendicular to the sample can be considered instantaneous. Compared with horizontal heat conduction, the vertical heat conduction of anisotropic materials like a graphite-sheet is considered to be less (Table I). To determine the thermal diffusivity perpendicular to the plane, the absorption length is required. However, absorption coefficient of graphite-sheet is unknown so that we assumed the length as 10^{-6} m same as graphite [7]. Then as a rough approximation, the thermal diffusivity perpendicular to the plane is estimated to be 7.9 $mm^2 \cdot s^{-1}$. This leads us to the conclusion that the DGR may be suited to measure high-conductive anisotropic materials such as graphite-sheet.

ACKNOWLEDGMENTS

The work described in this paper was financially supported in part by the Science and Technology Agency under a Promotion System for Intellectual Infrastructure of Research and Development.

REFERENCES

1. J. E. Graebner, *Rev. Sci. Instrum.*, **66**:3903 (1995).
2. T. Ushiku, Y. Taguchi and Y. Nagasaka, *Proc. 36th Natl. Heat Transf. Symp. Jp.*, 699 (1999).
3. Y. Taguchi and Y. Nagasaka, *Proc. 37th Natl. Heat Transf. Symp. Jp.*, (to be published) (2000).
4. H. S. Carslaw and J. C. Jaeger, *Conduction of Heat in Solids*, 2nd ed., (Oxford Univ. Press, London, 1959), pp. 353 - 362.
5. J. A. Nelder and R. Mead, *Comp. J.*, **7**:308 (1965).
6. T. Hoshi and M. Murakami, *National Technical Report*, **40**:74 (1994).
7. E. D. Palik, *HANDBOOK OF OPTICAL CONSTANTS OF SOLIDS* II, (Academic Press, Boston, 1991), pp. 449 - 460.

Table I. The specifications of graphite-sheet.

Thermal conductivity	$\lambda_{//}$: 600 ~ 1000 ($W \cdot m^{-1} \cdot K^{-1}$) $\lambda_{\perp}$: 5 ($W \cdot m^{-1} \cdot K^{-1}$)
Density	about 1.0 ($g \cdot cm^{-3}$)
Thickness	about 0.1 (mm)

LIST OF FIGURE CAPTIONS

Fig. 1 The principle of DGR. (a) Ideal case for one-dimensional heat conduction parallel to the plane. (b) Ideal case for one-dimensional heat conduction perpendicular to the plane.

Fig. 2 The ideal temperature distribution of grating.

Fig. 3 A typical example of two temperature decay outputs when the detection spot is located on a peak and valley with transient thermal grating which is detected by scanning. The sample is 0.05 mm-thick Zr foil. Λ = 332mm.

Fig. 4 Experimental apparatus of DGR.

Fig. 5 Non-dimensional temperature change T_x coresponding to the data in Fig. 3.

Fig. 6 The quadratic dependence of time constant on fringe space.
The thermal diffusivity parallel to the plane is calculated 10.3 $mm^2 \cdot s^{-1}$ from the slope.

Fig. 7 The quadratic dependence of time constant on fringe space.
The thermal diffusivity parallel to the plane is calculated 602 $mm^2 \cdot s^{-1}$ from the slope.

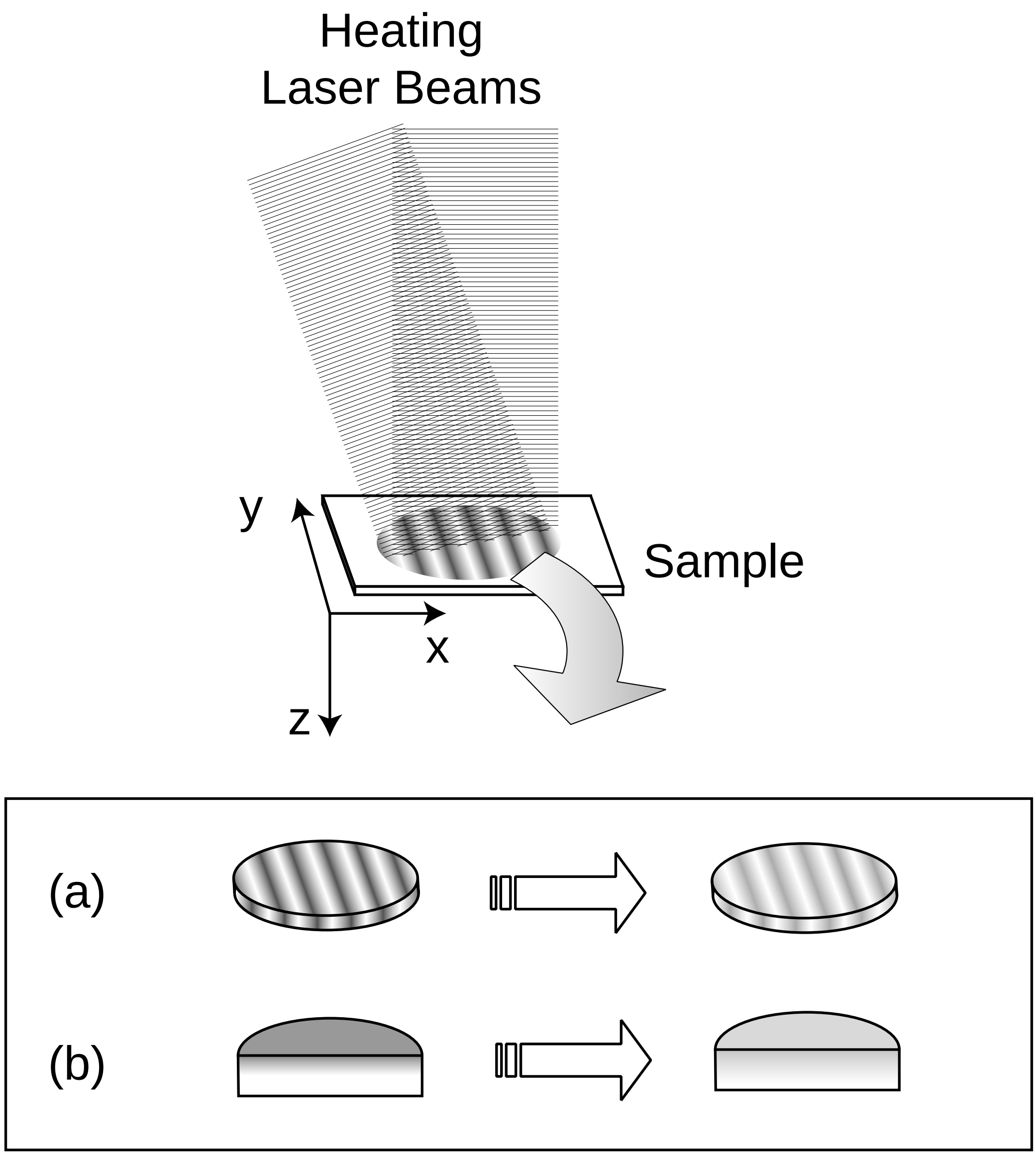

Heating
Laser Beams
y
Sample
x
z
(a)
(b)

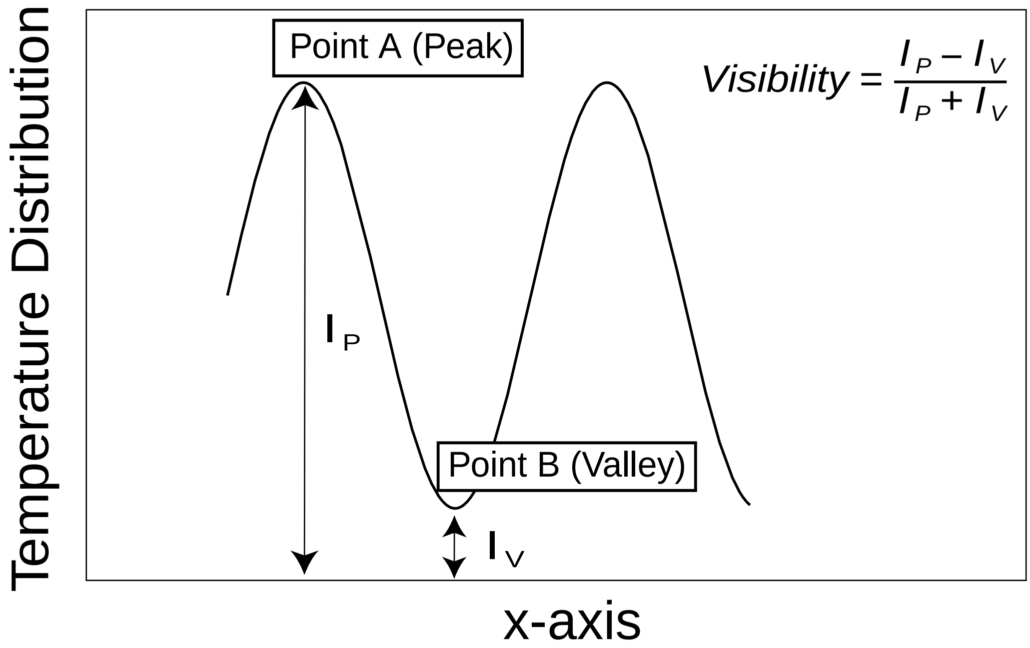
Point A (Peak)
Visibility = (I_P – I_V) / (I_P + I_V)
I_P
Point B (Valley)
I_V
Temperature Distribution
x-axis

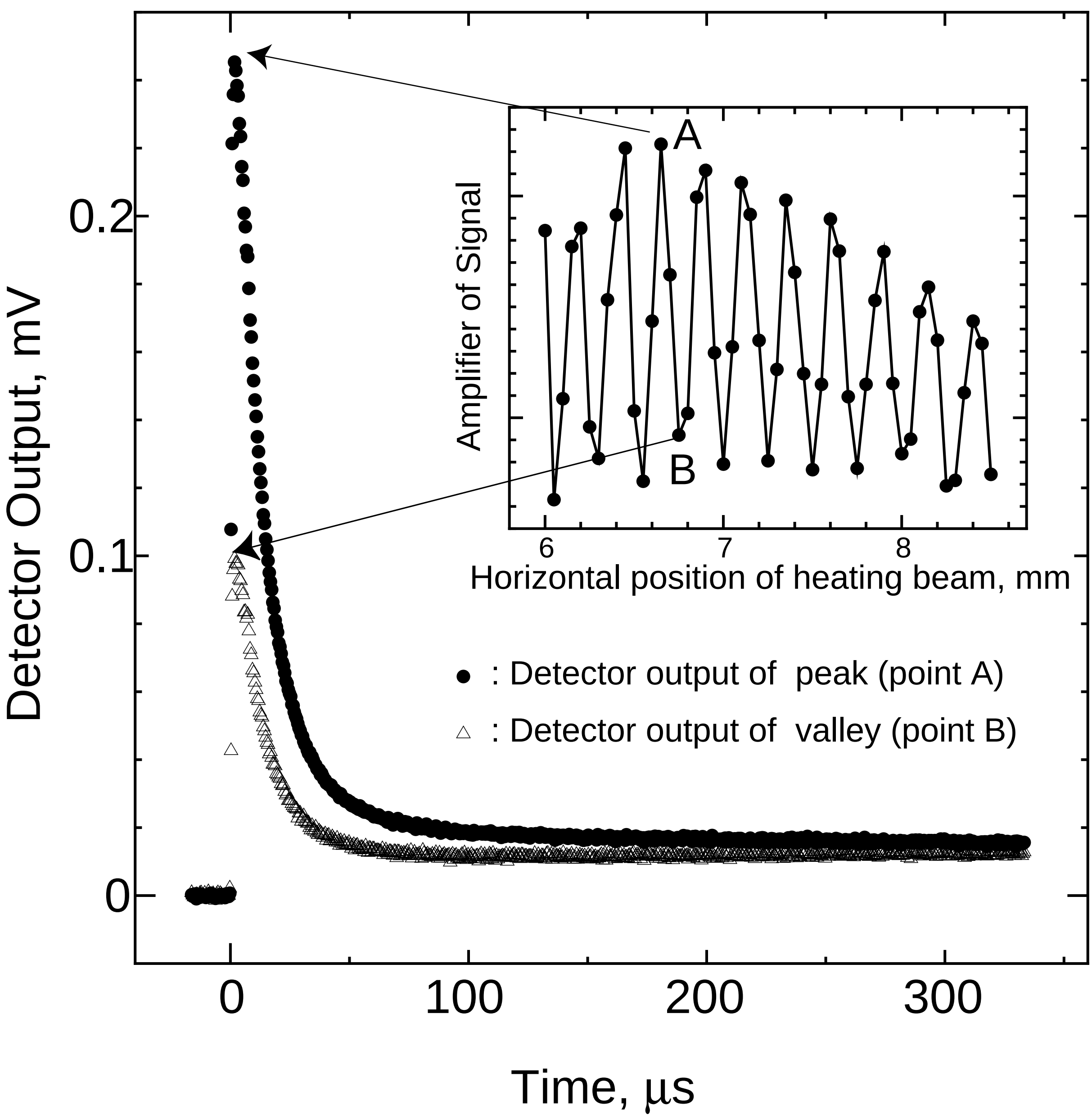

Detector Output, mV
0.2
0.1
0
0
100
200
300
Time, μs
A
B
Amplifier of Signal
6
7
8
Horizontal position of heating beam, mm
: Detector output of peak (point A)
: Detector output of valley (point B)

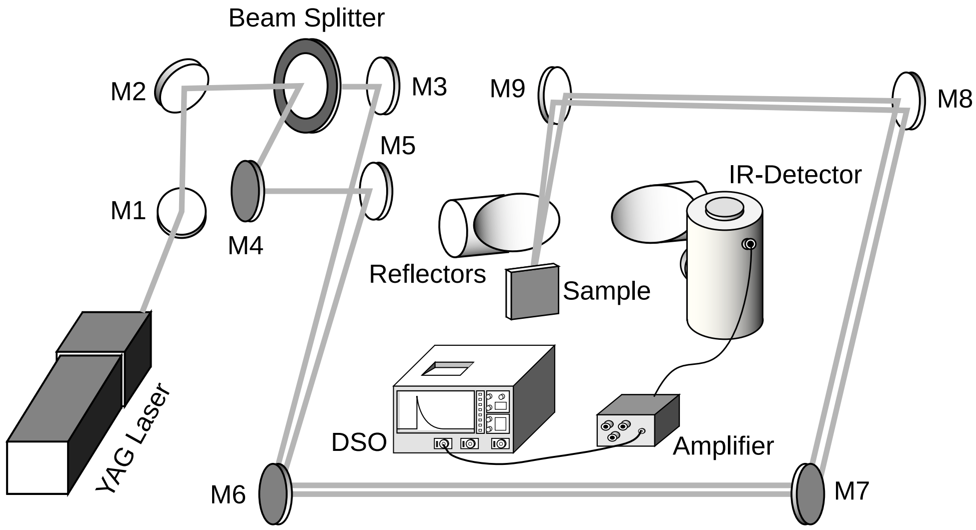
Beam Splitter
M2
M3
M9
M8
M5
M1
M4
IR-Detector
Reflectors
Sample
YAG Laser
DSO
Amplifier
M6
M7

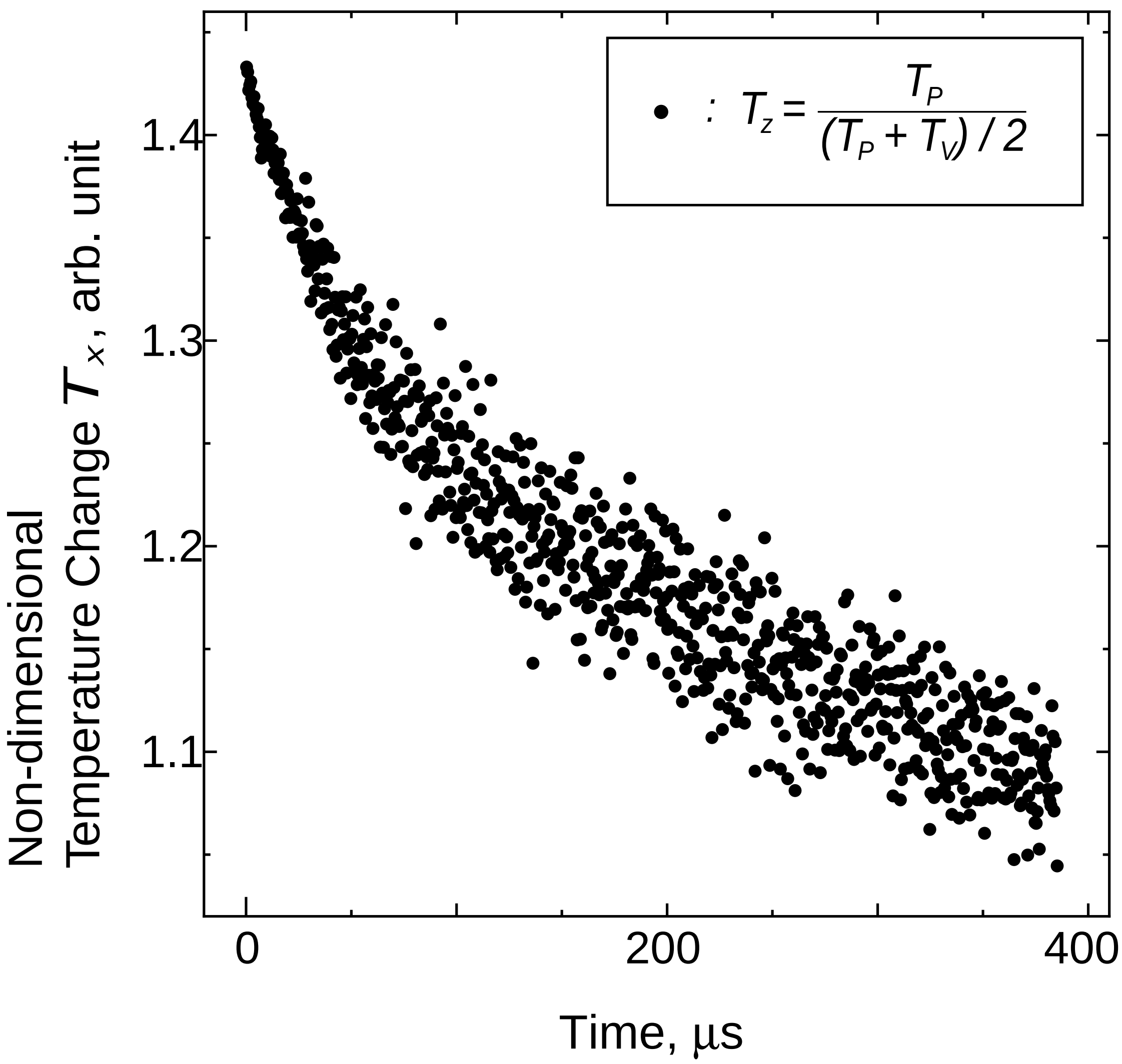

Non-dimensional Temperature Change T_x, arb. unit
1.4
1.3
1.2
1.1
0
200
400
Time, μs
$: T_z = \frac{T_P}{(T_P + T_V)/2}$

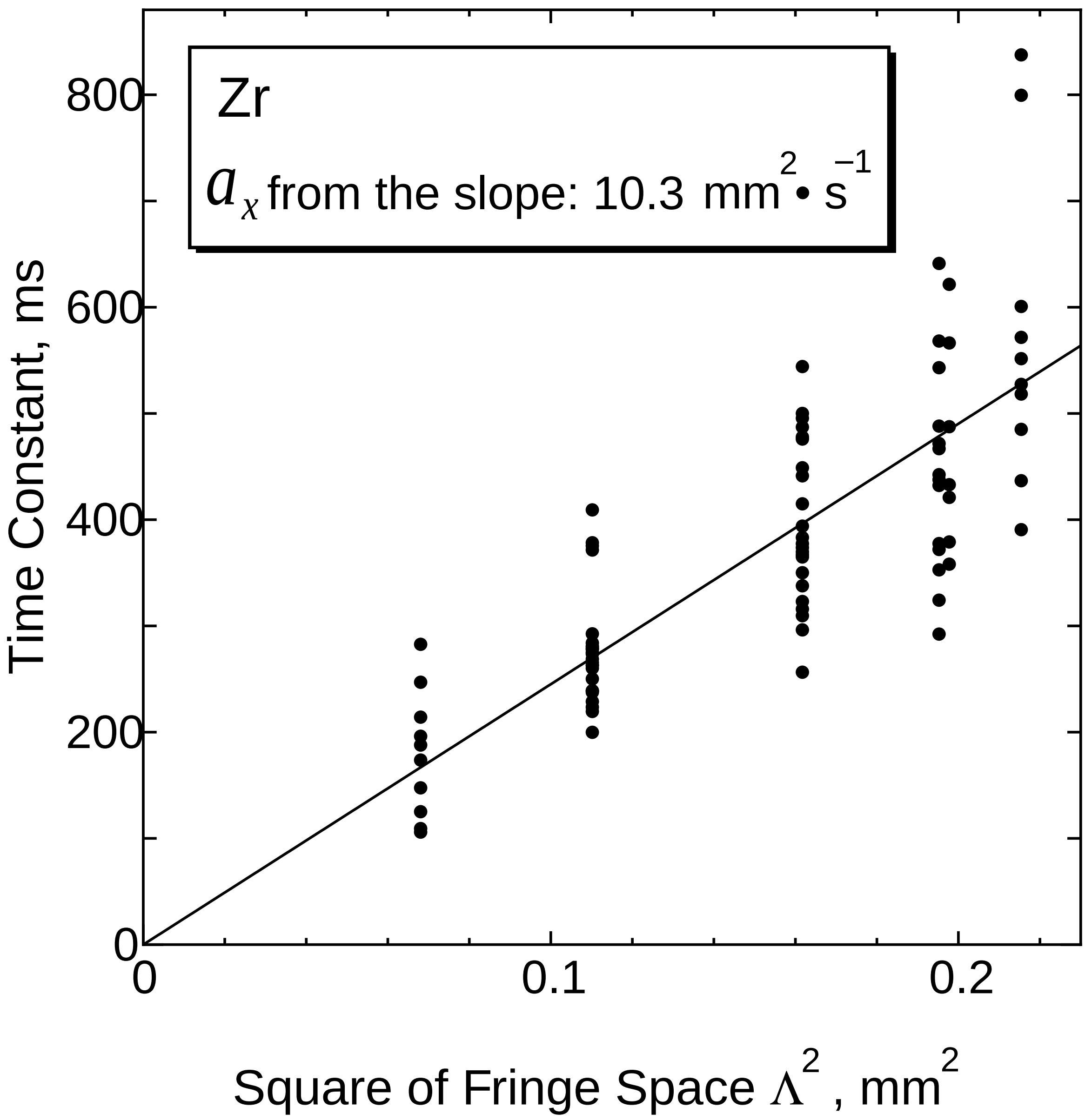

Zr
a_χ from the slope: 10.3 $mm^2 \cdot s^{-1}$
Time Constant, ms
800
600
400
200
0
0
0.1
0.2
Square of Fringe Space Λ^2, mm^2

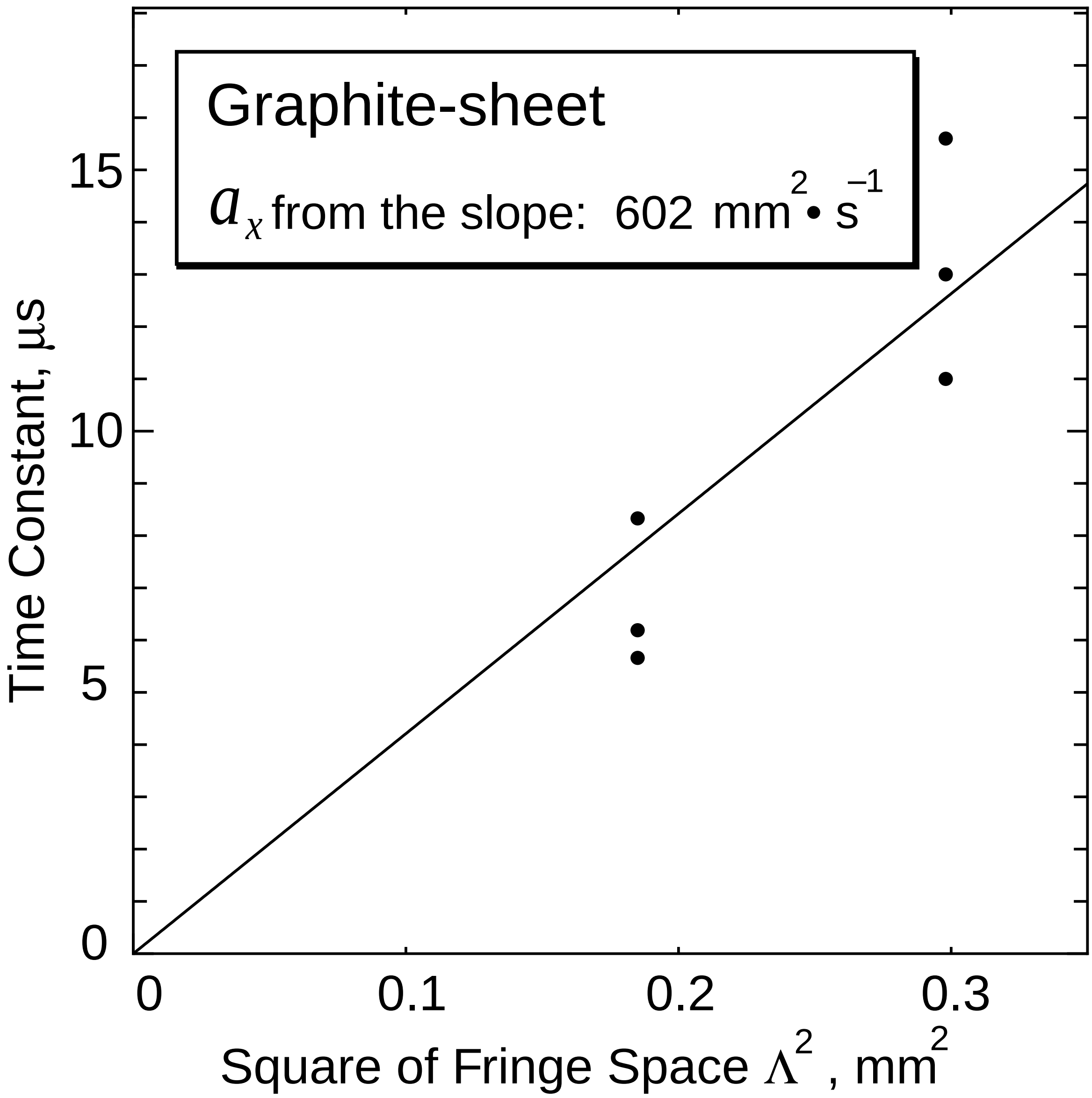

Graphite-sheet
a_x from the slope: 602 $mm^2 \cdot s^{-1}$
Time Constant, μs
0
5
10
15
0
0.1
0.2
0.3
Square of Fringe Space Λ^2 , mm^2